MOLECULAR REPRODUCTION AND DEVELOPMENT 67:233–242 (2004)

Oocyte Maturation in *Xenopus laevis* Is Blocked by the Hormonal Herbicide, 2,4-Dichlorophenoxy Acetic Acid

BARBARA STEBBINS-BOAZ,* KATHERINE FORTNER, JESSIE FRAZIER, SUZANNE PILUSO, SAMUEL PULLEN, MELISSA RASAR, WILLIAM REID, KRISTIN SINCLAIR, AND ELISA WINGER
Department of Biology, Willamette University, Salem, Oregon

ABSTRACT Oocyte maturation is dependent on a complex program of morphological, ultrastructural, and biochemical signaling events, and if disrupted could lead to decreased fertility and population decline. The in vitro sensitivity of amphibian oocytes and oocyte maturation to plant growth factor and widely used hormonal herbicide, 2,4-dichlorophenoxyacetic acid (2,4-D), was examined in this study to determine its potential impact on early development and possible contribution to the global amphibian decline. Progesterone, which acts through a membrane receptor, triggers meiotic maturation in full grown (stage VI) *Xenopus* oocytes, characterized by cytoskeletal reorganization, nuclear dissolution, chromosome condensation, and spindle formation. Biochemically, the Mos/MAPK/MPF signaling pathway is activated, in part dependent on translational activation of specific maternal mRNAs such as c-Mos. Light microscopy revealed unusual asymmetric morphotypes in oocytes exposed to 2,4-D alone characterized by a white spot and bulge, termed coning, in the animal pole where the germinal vesicle (nucleus) persisted intact. Treatment of oocytes with cytochalasin B, a microfilament inhibitor, blocked these morphotypes but nocodazole, a microtubule depolymerizing agent, did not. Confocal microscopy showed that 2,4-D, itself, caused substantial depolymerization of perinuclear microtubules. Importantly, 2,4-D blocked progesterone-induced maturation as measured by the lack of nuclear breakdown, confirmed by the lack of Mos expression, MPF activation, and cytoplasmic polyadenylation of cyclin B1 mRNA. However, Western blot analysis and U0126 inhibitor studies showed that 2,4-D, either alone or in the presence of progesterone, induced MAPK phosphorylation through MAPKK. These results show that 2,4-D disrupts oocyte cytoskeletal organization and blocks maturation while stimulating an independent MAPK signaling pathway. *Mol. Reprod. Dev. 67: 233–242, 2004.* © 2004 Wiley-Liss, Inc.

Key Words: cytoskeleton; Mos; MAPK; MPF; cytoplasmic polyadenylation; cyclin B1

INTRODUCTION

The differentiation of germ cells is fundamental to the reproductive health and continuity of all animals. Importantly, the egg provides many of the localized maternal proteins and mRNA necessary for embryonic cleavage divisions, axes formation, body plan and differentiation that follow fertilization. In the amphibian, *Xenopus laevis*, egg formation occurs through meiotic maturation of the full grown (stage VI) oocyte. A series of well-characterized ultrastructural and biochemical events are stimulated by progesterone that advance the cell cycle from prophase I to metaphase II, where the mature oocyte (egg) arrests until fertilization. Chromosomes condense, the meiotic spindle forms, and the germinal vesicle (nucleus) breaks down (GVBD), which produces a visible white spot in the pigmented animal pole often used as a visual marker for maturation (Hausen and Riebesell, 1991; Ferrell, 1999).

Progesterone induces changes in the oocyte through a membrane receptor-mediated signal transduction pathway (Masui and Markert, 1971; Smith and Ecker, 1971), though, recently, a classical predominantly cytosolic progesterone receptor from *Xenopus* oocytes has been cloned (Bayaa et al., 2000; Tian et al., 2000). Several of the key signaling events include synthesis of the serine/threonine kinase, Mos, which activates MAPK (ERK2) through MAPKK (MEK) (Resing et al., 1995). MAPK indirectly stimulates M-phase promoting factor, MPF, the p34cdc2/cyclin B heterodimer (Kosako et al., 1994), resulting in GVBD. Maturation requires protein synthesis. Key cell cycle regulators, such as Mos and cyclin B, are synthesized from stored maternal mRNAs,

Grant sponsor: Murdock Charitable Trust (to B.S.-B.); Grant sponsor: Willamette University (including Atkinson Faculty Development Awards); Grant sponsor: Science Collaborative Research Program.

*Correspondence to: Barbara Stebbins-Boaz, Department of Biology, Willamette University, Salem, OR 97301.
E-mail: bstebbin@willamette.edu

Received 30 May 2003; Accepted 3 September 2003
Published online in Wiley InterScience (www.interscience.wiley.com).
DOI 10.1002/mrd.10396

which undergo translational upregulation by cytoplasmic poly(A) elongation of their 3′ ends (Stebbins-Boaz et al., 1996; Stebbins-Boaz and Richter, 1997; Mendez and Richter, 2001).

Interest in factors that either mimic, promote, or block hormonally induced events, known as endocrine disrupters, has increased as accumulating evidence suggests that many agricultural and industrial chemicals introduced into the environment have unintended consequences on animal development and reproduction (Schettler et al., 1999). 2,4-Dichlorophenoxyacetic acid (2,4-D) is one of the most commonly used agricultural, commercial, and domestic herbicides (Lilienfeld and Gallo, 1989). A member of the phenoxy herbicides, 2,4-D resembles an auxin, a type of natural plant growth hormone (Gaspar et al., 1996). Auxins promote growth, cell division and differentiation through mechanisms that likely involve MAPK signaling, though these are not yet well characterized (Sitbon and Perrot-Rechenmann, 1997; Morris, 2001).

Because of the high potential of nontarget species exposure to 2,4-D through contamination of water, soil and air, a large number of animal and in vitro studies have investigated its mode of toxicity (Bradberry et al., 2000). The effects of 2,4-D on early development are unknown, but if negative, it could be a contributing factor to the global amphibian population decline. Given the difficulties of in vivo examination of gonadal tissue and its long-term reproductive health, we have addressed this issue by examining the in vitro response of full-grown *Xenopus* oocytes to 2,4-D. Our results demonstrate that 2,4-D induces significant morphological, cytoskeletal, and biochemical responses in oocytes as well as prevents progesterone-induced maturation.

MATERIALS AND METHODS

Oocyte Isolation

Ovariectomies were performed on anesthetized *Xenopus laevis* females (Xenopus Express, Inc., Plant City, FL). Ovary fragments were defolliculated enzymatically by gently shaking in a mixture of collagenase (2 mg/ml final) and dispase (1.2 mg/ml final) in modified Barth's saline (MBS) (88 mM NaCl, 1 mM KCl, 0.33 mM $Ca(NO_3)_2 \cdot 4H_2O$, 0.41 mM $CaCl_2 \cdot 2H_2O$, 0.82 mM $MgSO_4 \cdot 7H_2O$, 2.4 mM $NaHCO_3$, 10 mM HEPES, pH 7.4), 1.5–2 hr at room temperature. Stage VI (largest) oocytes were manually selected and allowed to equilibrate in MBS, pH 7.4, overnight at 17°C.

Oocyte Treatments

Equilibrated oocytes were transferred to MBS adjusted to pH 6.8 to which was added the indicated treatments. Progesterone (Sigma, St. Louis, MO), dissolved in ethanol, was added to a final concentration of 10 μM. 2,4-D, sodium salt (Sigma), dissolved in water, was added to a final concentration of 10 mM, unless otherwise stated, and oocytes were incubated at room temperature for the indicated times. In some cases, progesterone and 2,4-D were added simultaneously to oocyte cultures. Cytochalasin B, colchicine and nocodazole (Sigma) and U0126 (Calbiochem, San Diego, CA) were dissolved in dimethylsulfoxide (DMSO) (Sigma). Oocytes were pre-incubated in final concentrations of 25 μg/ml cytochalasin (Gard et al., 1995); 20 μg/ml nocodazole (Gard et al., 1997), 50 μM U0126 (Gross et al., 2000), 0.1% dimethylsulfoxide (DMSO); or 50 μg/ml cycloheximide (CHX) (Sigma) (dissolved in ethanol) for 1 hr at room temperature. The percentage white spot or coning was recorded at the indicated time-points. Otherwise oocyte collection occurred at 50% white spot formation which was approximately 4–6 hr after addition of progesterone or 2,4-D. Oocytes were either immediately frozen at −80°C for later analysis or fixed and stained for confocal immunofluorescence microscopy. All experimental and control conditions contained at least 30 oocytes and were repeated at least three times.

Detection of Microtubules by Confocal Scanning Laser Microscopy

Oocytes were fixed and stained for microtubules according to Danilchik (personal communication). Oocytes were fixed in 3.7% formaldehyde, 0.25% glutaraldehyde, 0.2% Triton X-100 in microtubule assembly buffer (MTAB) (80 mM K-PIPES, pH 6.8, 5 mM EGTA, 1 mM $MgCl_2$) for 2–4 hr at room temperature or overnight at 4°C. Oocytes were then post-fixed in absolute methanol overnight at −20°C, bleached in 10% hydrogen peroxide/67% methanol for 2–6 hr on a light box, and rehydrated in three consecutive 10 min rinses in 50% methanol/50% TBS (155 mM NaCl, 10 mM Tris-HCl, pH 7.4), 25% methanol/75% TBS, 100% TBS. Oocytes were then incubated in TBS containing 100 mM $NaBH_4$ for 4 hr at room temperature or overnight at 4°C to reduce yolk platelet autofluorescence. After washing five times, 10 min each in TBSN (TBS with 0.1% Nonidet P-40), oocytes were bisected along the animal-vegetal axis and incubated overnight at 4°C in 1:1,000 dilution of mouse anti-α- and β-tubulin antibody (Biogenesis, Kingston, NH, Cat no.: 9280-0504) in FBS (TBS containing 10% fetal bovine serum (Sigma) and 5% DMSO). After washing in TBSN, five times, 1 hr each, oocytes were incubated in 1:100 dilution of Alexa Fluor 546 goat anti-mouse IgG secondary antibody (Molecular Probes, Eugene, OR, Cat no.: A-11003) and then washed as above. Oocytes were dehydrated in two rinses, 30–60 min each, of absolute methanol and cleared in 2 rinses, 30 min each, of Murray's Clear (2:1, benzyl benzoate:benzyl alcohol (Sigma)). Oocytes were mounted in depression slides in Murray's Clear and examined with a Bio-Rad laser scanning confocal microscope attached to a Nikon laser unit. Optical section thickness ranged from 1–4 μm.

Oocyte Homogenates and Western Blot Analysis

Oocytes were homogenized by pipetting in 10 μl/oocyte of Homogenization buffer (HB) (0.1 M KCl, 1 mM $MgCl_2$, 50 mM Tris-HCl (pH 7.5), 1 mM DTT, 80 mM

β-glycerophosphate, 10 μg/ml leupeptin, chymopeptin, pepstatin). After pelleting homogenates by centrifugation at 10,000 rpm, 10 min at 4°C, supernatants were mixed with 2× SDS loading buffer (2% sodium dodecylsulphate, 20% glycerol, 0.72 M β-mercaptoethanol, 125 mM Tris-HCl, pH 6.8, 0.001% bromophenol blue) and heat denatured for 10 min at 95°C. Each sample contained five oocytes and approximately 0.8 oocyte equivalent was further analyzed.

Proteins were fractionated by Sodium docecyl sulfate–polyacrylamide electrophoresis (SDS–PAGE) using standard techniques (Ausubel et al., 1997) and electroblotted onto nitrocellulose in 10 mM CAPS, pH 11 using a Hoeffer Semiphor according to the manufacturer's instructions (Amersham Pharmacia Biotech, Newark, NJ). Membranes were rinsed once in distilled water and proteins were stained in 0.1% Ponceau S, 5% acetic acid. After blocking in 5% nonfat milk in TBST (0.15 M NaCl, 10 mM Tris, pH 8, 0.05% polyoxyethylenesorbitan monolaurate (Tween-20) (Sigma)) for 1 hr at room temperature while shaking, membranes were incubated in a 1/1,000 dilution of the indicated primary antibody (with the exception of Mos antibody, see below) in 5% milk, TBST for 1 hr at room temperature, washed four times in TBST for 5 min each with shaking, followed by 1 hr at room temperature in a 1/2,000 dilution of secondary antibody. MAPK was detected with ERK 2 (C-14) goat polyclonal antibody (Santa Cruz Biotech, sc-154) followed by donkey anti-goat IgG conjugated to HRP (Santa Cruz, CA). Tyrosine phosphorylated MAPK (*Xenopus* residue tyr 190) was detected with P-ERK (E-4) mouse monoclonal antibody (Santa Cruz Biotech, sc-7383) followed by HRP-conjugated anti-mouse antibody (Amersham Life Sciences). Mos was detected by incubating in a 1/500 dilution of Mos^{Xe} (C237) rabbit polyclonal antibody (Santa Cruz Biotech, sc-86) overnight at 4°C, followed by a 1/2,000 dilution of HRP-conjugated anti-rabbit IgG. Immunoreactive proteins were visualized by chemiluminescence using the ECL Western blotting reagents according to the manufacturer's instructions (Amersham Biosciences Corp., Piscataway, NJ) and autoradiography.

H1 Kinase Assay

Histone H1 kinase assays were performed according to Nebreda and Hunt (1993). Oocytes were homogenized at 20 μl/oocyte in H1 kinase buffer (160 mM sodium β-glycerophosphate, 40 mM EGTA, 30 mM $MgCl_2$) supplemented with a final concentration of 0.5 mM sodium orthovanadate, and 10 μg/ml leupeptin and chymostatin. Homogenates were centrifuged at 10,000 rpm for 5 min at 4°C. To 8 μl of supernatant, 4 μl of histone mix (0.5 mg/ml histone H1 Type III S (Sigma), 2 μCi γ-^{32}P-ATP (3,000 Ci/mM) (NEN, Boston, MA)) were added and incubated at room temperature for 15 min. Each sample was diluted with an equal volume of 2× SDS loading buffer and heat denatured at 95°C for 10 min. Samples were fractionated by SDS–PAGE using a 12% running gel and radiolabeled histone H1 was visualized by autoradiography.

RNA Extraction and Northern Blot Analysis

Oocytes were homogenized at 50 μl/oocyte in TNES-proteinase K buffer (100 mM Tris-HCl, pH 7.5, 300 mM NaCl, 10 mM EDTA, 2% (w/v) SDS, 200 μg/ml proteinase K (Sigma)). After incubation for 1 hr at 50°C, RNA was extracted with 1:1 phenol:chloroform followed by ethanol precipitation. Total RNA was dissolved directly in Northern loading buffer (61% formamide, 7.2% formaldehyde, 4.8% glycerol, 0.3 M boric acid, 30 mM sodium borate, 60 mM sodium sulfate, 6 mM EDTA, 0.1% bromophenol blue, 0.1% xylene cyanol, supplemented with ethidium bromide (final 0.025 mg/ml), and heat denatured for 5 min at 100°C. RNA samples were resolved by denaturing gel electrophoresis in a 1% agarose, 3% formaldehyde gel in 1× Northern running buffer (50 mM boric acid, 5 mM sodium borate, 10 mM sodium sulfate, 1 mM EDTA), transferred to nylon by capillary action in 10× SSC (1.5 M NaCl, 0.15 M trisodium citrate-$2H_2O$, pH 7) using standard procedures (Ausubel et al., 1997). A 1.4-kbp fragment was isolated from a *Xenopus* cyclin B1 cDNA construct as described (Stebbins-Boaz et al., 1996), purified from low melt agarose (Ausubel et al., 1997) and labeled using the DIG High Prime DNA Labeling and Starter Kit (Roche Diagnostics, Chicago, IL). Conditions for probe hybridization and detection were performed according to the manufacturer's instructions.

RESULTS

2,4-D Induces Morphological Effects but no GVBD

Because 2,4-D is a plant growth regulator, we suspected that it had the potential to influence the oocyte, in particular the cell cycle or maturation. In order to test this, full-grown *Xenopus* oocytes were incubated in various concentrations of 2,4-D with or without progesterone and scored for white spot formation (WSF), an often used marker of meiotic maturation (Fig. 1). As expected, control oocytes in buffer alone (Fig. 1A,D) showed no change up to 10 hr while a majority in progesterone underwent WSF indicative of maturation (Fig. 1B,D). Interestingly, 2,4-D-treated oocytes also underwent WSF at rates similar to those exposed to progesterone (Fig. 1D). We found that oocytes were most sensitive to a final concentration of 10 mM 2,4-D at pH 6.8 (data not shown). Assuming that, as shown by others (Charles et al., 2001), the protonated form of 2,4-D is the active agent, then its actual concentration at pH 6.8 is calculated at 156 μM. It is noteworthy that other in vitro systems responded to similar concentrations of 2,4-D (Zhao et al., 1987; Rosso et al., 2000; Kaioumova et al., 2001; Tuschl and Schwab, 2003).

Although WSF is a useful preliminary indication of maturation, it does not necessarily reflect genuine germinal vesicle breakdown (GVBD). To determine whether 2,4-D did indeed induce meiotic maturation, we manually dissected oocytes and scored for the absence or presence of intact GVs (data not shown).

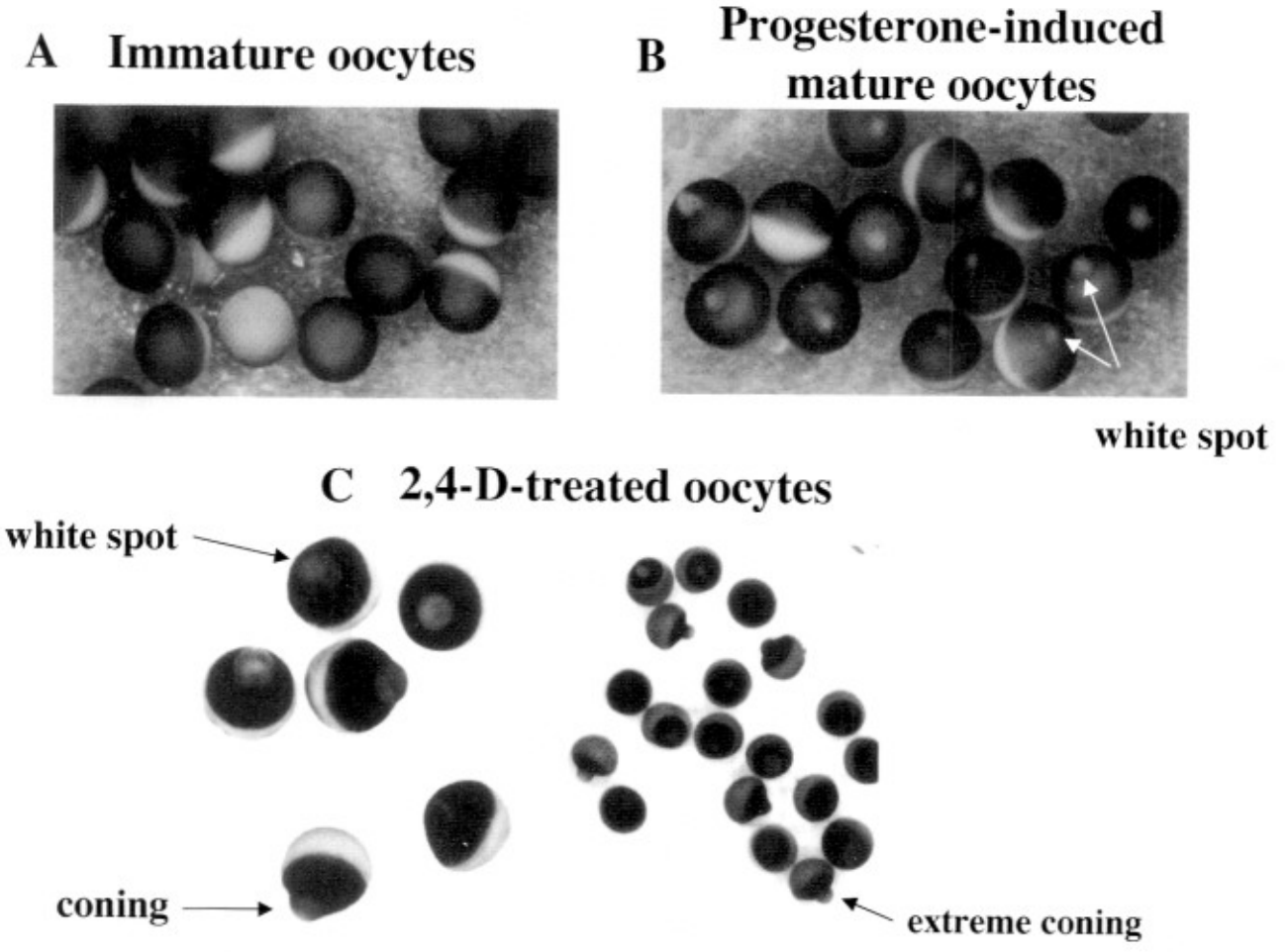
A Immature oocytes
B Progesterone-induced mature oocytes
white spot
C 2,4-D-treated oocytes
white spot
coning
extreme coning
D
Buffer
Progesterone
2,4-D
% White spot/Coning
Exposure Time (hours)
0
10
20
30
40
50
60
70
80
90
100
1
2
3
4
5
6
7
8
9
10

Fig. 1.

Oocytes incubated in buffer alone had intact GVs while progesterone-treated oocytes lacked GVs, as expected. 2,4-D-treated oocytes, on the other hand, contained visually intact GVs (data not shown). This was confirmed by confocal microscopy (Fig. 2G,K). These results indicate that 2,4-D did not, in fact, induce true meiotic maturation. Furthermore, approximately 1 hr following white spot formation, a majority of 2,4-D-treated oocytes became asymmetric in shape and displayed a bulge or cone coincident with the white spot in the animal pole (Fig. 1C). Manual dissection revealed the presence of the GV within the cone. These morphological responses suggested that 2,4-D influences cytoskeletal organization, which determines GV localization and membrane contour.

2,4-D Perturbs the Cytoskeleton

To determine whether 2,4-D perturbed the cytoskeleton, we examined microtubules directly by confocal immunofluorescence microscopy. Oocytes treated with 2,4-D were fixed and incubated with anti-α/β-tubulin antibody followed by a fluorescently labeled secondary antibody, and subjected to confocal immunofluorescence microscopy (Fig. 2). Untreated oocytes showed a dense network of microtubules around the GV (Fig. 2C,D). Progesterone-induced mature oocytes, having undergone GVBD, lacked significant staining with the exception of the meiotic spindle and polar body located adjacent to the plasma membrane in the animal pole (Fig. 2E,F). As a negative control, oocytes were treated with nocodazole, a known microtubule destabilizer, and as expected, staining around the nucleus was dramatically diminished and more diffuse compared to untreated oocytes (Fig. 2I). Magnification of the perinuclear region revealed a speckled fluorescent pattern indicative of short, depolymerized microtubules (Fig. 2J). A similar pattern was observed around the intact GV of 2,4-D-treated oocytes at low (Fig. 2G) and high magnification (Fig. 2H). Furthermore, oocytes incubated in both progesterone and 2,4-D clearly did not undergo GVBD but did display microtubule depolymerization (Fig. 2K,L). These results show that 2,4-D alone does not induce GVBD but in fact blocks it in the presence of progesterone. In addition it stimulates microtubule depolymerization, which may in part be responsible for changes in oocyte morphology and nuclear localization.

To address whether 2,4-D-induced morphologies were dependent on the cytoskeleton, oocytes were preincubated in nocodazole or cytochalasin B, a microfilament disrupter. 2,4-D was then added and the percentage white spot and coning were observed (Fig. 3). Progesterone-induced white spot was unaffected by

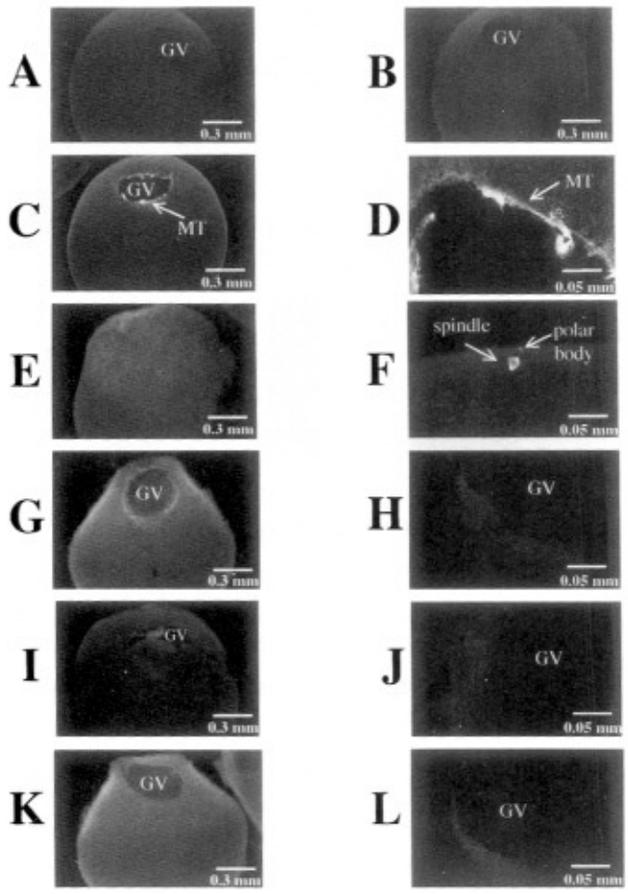

Fig. 2. 2,4-D causes depolymerization of perinuclear microtubules (MT) in oocytes. Oocytes were treated as indicated below, fixed and immunostained with anti-tubulin antibody as described in "Materials and Methods." Immunofluorescent images of MT were obtained by confocal laser scanning microscopy. **A**: Control: oocyte incubated in buffer alone; immunostaining with 1° but not 2° antibody. **B**: Control: oocyte incubated in buffer alone, immunostaining with 2° but not 1° antibody. **C**: Control: oocyte incubated in buffer alone and fully immunostained with both 1° and 2° antibodies. Note: bright perinuclear staining. **D**: Same as (C) but perinuclear region is magnified six times. **E**: Progesterone-treated oocyte fully immunostained. Note: lack of GV due to GVBD. **F**: Same as (E) but region of meiotic spindle and polar body is magnified six times. **G**: 2,4-D-treated oocyte fully immunostained. Note: presence of GV, diffuse staining and cone morphology. **H**: Same as (G) but perinuclear region is magnified six times. Note: speckled staining pattern. **I**: Nocodazole-treated oocytes fully stained. Note: presence of GV, and diffuse staining. **J**: Same as (I) except perinuclear region is magnified six times. Note: speckled staining pattern. **K**: Oocytes co-incubated in progesterone and 2,4-D, fully stained. Note: presence of GV, diffuse staining, and cone morphology. **L**: Same as (K) except perinuclear region is magnified six times. Note: speckled staining pattern. GV (germinal vesicle) and size scales are indicated in each image.

Fig. 1. Morphological responses of stage VI oocytes to progesterone and 2,4-D. **A**: Immature oocytes incubated in buffer alone. Note that each oocyte is bipolar with an unpigmented vegetal and pigmented animal hemisphere. **B**: Oocytes incubated in 10 μm progesterone. Arrows label the white spot indicative of germinal vesicle breakdown and maturation. **C**: Oocytes incubated in 10 mM 2,4-D. Arrows label the white spot and cone. **D**: Bar graph depicting typical morphological responses over time. None to few oocytes developed white spots or cones in buffer alone (filled bars); progesterone-treated oocytes showed white spot, only (unfilled bars); 2,4-D-treated showed white spot that subsequently developed into a cone (lined bars). Sibling oocytes (100–150) were observed for each treatment. The experiment was performed at least three times with similar trends using oocytes from different females.

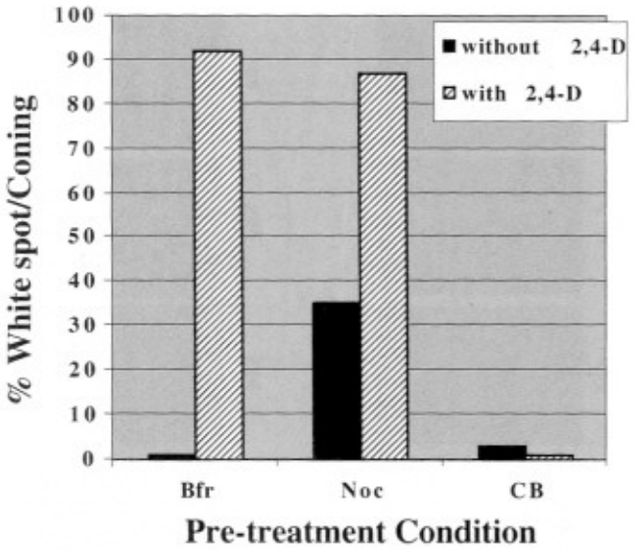

Fig. 3. Cytochalasin B but not nocodazole blocks 2,4-D-induced white spot and coning. Data are shown from a typical experiment where 30–50 sibling oocytes were pre-treated as indicated and then incubated without (filled bars) or with (lined bars) 2,4-D and scored for white spot or coning. Buffer, bfr; Nocodazole, Noc; Cytochalasin B, CB. The experiment was repeated at least five times with oocytes from different females with similar trends.

either chemical (data not shown), although pre-treatment with cytochalasin produced a more diffuse white spot, as previously documented (Gard et al., 1995). While the percentage of 2,4-D-induced white spot and coning were unchanged by nocodazole (about 90%), it was dramatically reduced by cytochalasin B to less than 4%. These results suggest that 2,4-D requires actin microfilaments to induce a morphological response. Both 2,4-D and nocodazole cause microtubule depolymerization; thus it cannot be excluded that microtubules are not also involved in these morphological effects. However, it is noteworthy that microtubule depolymerization by nocodazole does not by itself strongly induce white spot formation (not more than 35%) and never coning, compared to over 85% white spot and coning in 2,4-D treated oocytes. Taken together, these results suggest that 2,4-D requires microfilaments to initiate the observed morphological effects.

2,4-D, Alone, Stimulates MAPK but Blocks the Progesterone Signal Transduction Pathway

To examine the biochemical effects of 2,4-D on oocytes and maturation, we looked at the Mos/MAPK/MPF signaling pathway. Some oocytes were incubated in progesterone, 2,4-D alone, or both. Oocytes were observed over time for the appearance of a white spot in progesterone-treated samples as well as for white spot and coning in 2,4-D-treated samples. Protein homogenates were prepared from responding oocytes, fractionated by SDS–PAGE and Mos expression was determined by Western blot analysis using anti-Mos antibody (Fig. 4). As expected, oocytes incubated in buffer alone underwent no visible change and did not

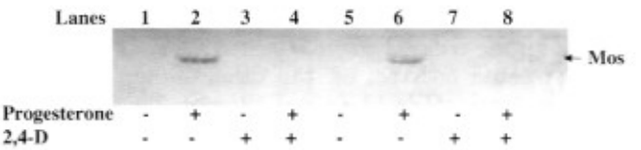

Fig. 4. 2,4-D blocks Mos protein expression. Protein homogenates from oocytes treated as indicated were fractionated by electrophoresis and Mos protein (arrow) detected by Western blot analysis. **Lanes 1–4** and **5–8** contain oocyte samples from two separate frogs. Absence or presence of progesterone (10 μM) or 2,4-D (10 mM) are indicated by –/+, respectively.

express Mos (Fig. 4, lanes 1 and 5), while oocytes incubated in progesterone formed a white spot and did express Mos (Fig. 4, lanes 2 and 6). Oocytes treated with 2,4-D with or without progesterone, also underwent white spot formation which typically progressed into a cone but did not express Mos (Fig. 4, lanes 4 and 8). These results show that 2,4-D does not induce Mos expression; furthermore, it blocks progesterone-induced Mos expression, a critical early step in the maturation signal transduction pathway.

MPF activity was tested by histone H1 kinase assays in extracts from oocytes treated as above. Radiolabeled H1, indicative of MPF activity, was fractionated by SDS–PAGE and visualized by autoradiography. Figure 5 shows that progesterone strongly stimulated MPF activity compared to untreated oocytes (lanes 1, 2 and 7, 8). However, MPF was not activated by any of the various 2,4-D concentrations ranging from 2.5 to 10 mM (Fig. 5, lanes 3–5). In addition, progesterone-induced MPF activation was blocked by 5 mM 2,4-D (Fig. 5, lanes 6 and 9). These data support that 2,4-D inhibits the progesterone signaling pathway at the level of MPF activation.

We also examined MAPK phosphorylation by Western blot analysis, and postulated that it would not be activated by 2,4-D. However, contrary to our hypothesis, MAPK phosphorylation was independently induced by 2,4-D in a dose-dependent manner (Fig. 6A, lanes 3–5). This was confirmed using antibodies specific for phosphorylated MAPK (Fig. 6B). Additionally, high levels of MAPK were detected in oocytes co-incubated in progesterone and 2,4-D (Fig. 6A,B, lane 8). As expected, unphosphorylated MAPK was present in all extracts regardless of maturation state (Fig. 6A). In its active form, MAPK is dually phosphorylated and thus migrates somewhat slower than the unphosphorylated

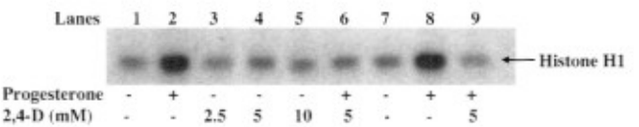

Fig. 5. 2,4-D inhibits MPF activation. Protein homogenates from oocytes treated as indicated were analyzed for Histone H1 kinase activity as described in "Materials and Methods." Samples were fractionated by electrophoresis and radiolabeled H1 (arrow) was visualized by autoradiography. Absence or presence of progesterone (10 μM) or 2,4-D are indicated by –/+, or numerically.

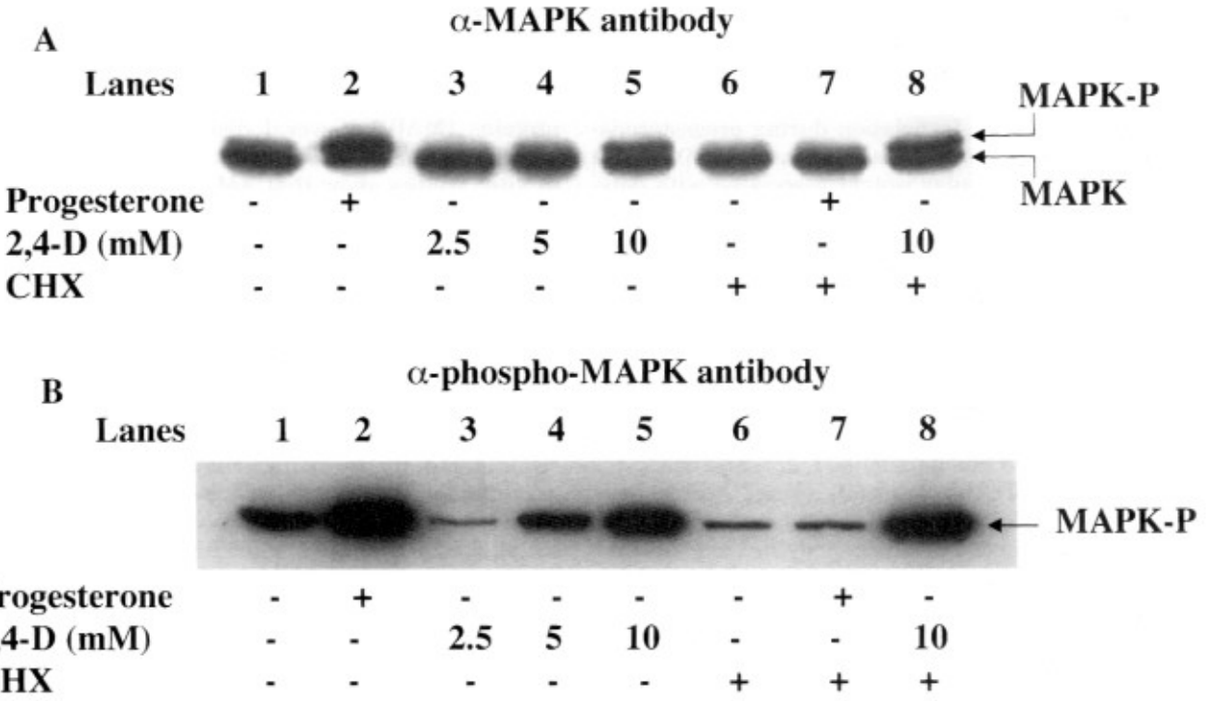

Fig. 6. 2,4-D induces MAPK activation independent of de novo protein synthesis. Protein homogenates from treated oocytes were fractionated and MAPK was detected by Western blot analysis. **A**: ERK-2 antibody was used to detect both phosphorylated (MAPK-P) and unphosphorylated MAPK, simultaneously. Samples were fractionated on a high resolution 15% running gel according to Chesnel et al. (1997). **B**: P-ERK antibody was used to detect phosphorylated MAPK only. Indicated oocytes (+) were pre-treated in CHX (cycloheximide) (50 μg/ml) for 1 hr prior to additional treatments which are identical to those in Figure 4.

form, detectable by high resolution SDS–PAGE. The doublet in Figure 6A, represents a mixture of active, phosphorylated (upper band), and inactive unphosphorylated (lower band) MAPK. As expected, MAPK in untreated immature oocytes (Fig. 6A, lane 1) shifts predominantly into the upper band in the presence of progesterone (Fig. 6A, lane 2). The combined data indicates that 2,4-D induces MAPK activation through a progesterone-independent pathway.

To determine whether 2,4-D-induced MAPK activation is dependent on protein synthesis, we pre-incubated oocytes in cycloheximide (CHX), followed by 2,4-D treatment and examined MAPK phosphorylation by Western blot analysis (Fig. 6). Although cycloheximide inhibited MAPK phosphorylation in progesterone-treated oocytes (Fig. 6A,B, lane 7), which is known to be dependent on protein synthesis, it did not inhibit MAPK phosphorylation in 2,4-D-treated oocytes (Fig. 6A,B, lane 8). These results provide further evidence that 2,4-D signaling through MAPK is distinct from the Mos/MAPK/MPF pathway in maturing oocytes and that it utilizes protein factors that are already present in the oocyte.

To test whether one of these factors was MAPKK (MEK), we asked whether a known inhibitor of MAPKK, U0126, would block MAPK phosphorylation in 2,4-D-treated oocytes. By Western blot analysis with a phosphospecific-MAPK antibody, we found that neither U0126 nor the solvent, DMSO, had any effect on the unphosphorylated state of MAPK in immature oocytes (Fig. 7, lanes 1–3). In contrast, U0126 blocked progesterone- and 2,4-D-induced MAPK phosphorylation (Fig. 7, lanes 5, 6 and 8, 9, respectively). These data indicate that the immediate upstream activator of MAPK in the 2,4-D-response is likely MAPKK.

2,4-D Inhibits Cytoplasmic Polyadenylation

Because 2,4-D alone neither stimulates Mos expression, which occurs from maternal mRNA stores, nor allows it in the presence of progesterone, we investigated whether other proteins whose mRNAs are

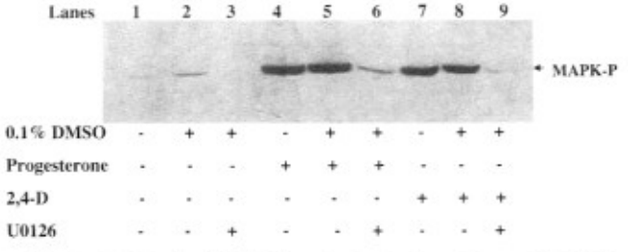

Fig. 7. 2,4-D-induced MAPK activation is dependent on MAPKK. Oocytes were pre-incubated for 1 hr in either DMSO or U0126 as indicated (+) prior to exposure to progesterone (10 μM) or 2,4-D (10 mM). Protein homogenates from treated oocytes were fractionated and analyzed by Western blot for the presence of phosphorylated

translationally controlled were also negatively affected by 2,4-D. In particular, we examined the cell cycle regulator, cyclin B1 mRNA. Like c-Mos mRNA, cyclin B1 mRNA undergoes a lengthening of its 3′ end by polyadenylation and translation during progesterone-induced maturation (Stebbins-Boaz et al., 1996). To test for changes in molecular weight associated with polyadenylation, total RNA was isolated from oocytes treated with progesterone and 2,4-D, fractionated by gel electrophoresis and analyzed by Northern blot with a labeled cyclin B1 cDNA probe. Figure 8 shows that two RNA species were detected as has been shown previously (Stebbins-Boaz et al., 1996). Maternal cyclin B1 mRNA is stored in the oocyte with a relatively short 3′ poly(A) tail, which is lengthened by polyadenylation into a slower migrating species during progesterone-induced maturation (Fig. 8, compare lanes 1, 2, 7, 8). For oocytes treated with 2,4-D, the faster migrating (shorter) form predominated (Fig. 8, lanes 3–5, 9–11). Furthermore, cyclin B1 mRNA remained primarily in the shortened form in oocytes co-incubated with progesterone and 2,4-D (Fig. 8, lanes 6 and 12). These data suggest that 2,4-D does not induce cytoplasmic polyadenylation on its own; moreover, it blocks this essential mechanism in progesterone-treated oocytes.

DISCUSSION

Oocyte maturation is a highly regulated mechanism that involves morphological, ultrastructural, and signaling events to ensure the successful generation of fertilizable eggs. Our results demonstrate that the hormone and herbicide, 2,4-D, has profound disruptive effects on oocyte structure and maturation in vitro. 2,4-D dramatically destabilizes microtubules surrounding the GV (Fig. 2). This could impact not only cell shape but also organellar and macromolecular localization and transport. For instance, the localization of important maternal transcripts such as VegT, required for germ cell formation (King et al., 1999) is dependent on microtubules. Our observations support previous work in other cell types. Zhao et al. (1987) show "cytoskeletotoxicity" in mouse 3T3 cells exposed to 2,4-D where microtubules and microfilaments display unusual bundling and aggregation. In other studies, neurite shortening is correlated with microtubule depolymerization in rat neurons cultured in the presence of 2,4-D (Rosso et al., 2000).

The regulation of microtubule assembly and dynamics are thought to be controlled by microtubule associated proteins (MAPs). Several distinct MAPs have been identified in *Xenopus* oocytes and eggs. In particular, in vitro studies show that XMAP230 stabilizes microtubules (Andersen et al., 1994). Immunofluorescence microscopy show that staining is strong for XMAP230 in *Xenopus* oocytes, particularly in the area surrounding the GV (Cha et al., 1998). With respect to our results, 2,4-D may destabilize microtubules by promoting the dissociation of XMAP230 from microtubules possibly through induction of MAPK-mediated phosphorylation. Shiina et al. (1992) showed that MAP kinase can phosphorylate XMAP230 in vitro, which results in its reduced affinity to microtubules and thus increased microtubule instability. Because microtubules are involved in nuclear positioning (Reinsch and Gönczy, 1998), 2,4-Ds disruptive effects may contribute to GV displacement toward the plasma membrane.

Although we would like to draw a causal link between 2,4-D-induced microtubule instability, and white spot and coning, the relationship may be complex as treatment with nocodazole alone, a known microtubule destabilizer, does not induce identical morphologies. Consequently, we postulate that 2,4-D has additional effects which, coupled with microtubule depolymerization, lead to the observed morphotypes. Because pretreatment of oocytes with cytochalasin B, an inhibitor of actin polymerization, blocks 2,4-D-induced morphotypes (Fig. 3), we believe that microfilaments are also required for oocyte sensitivity to 2,4-D. Previous studies have shown that two layers of microfilaments exist in the oocyte. The more superficial layer, or cortical layer, is sensitive to cytochalasin B (Merriam et al., 1983; Ryabova and Vassetzky, 1997). Given our data, it is likely that a component(s) of the cortical layer is important for the 2,4-D response. One possibility is that 2,4-D stimulates contraction or remodeling of the cortex which could lead to a juxtaposition of the unanchored GV against the plasma membrane, pigment reorganization (white spot), and distortion of the plasma membrane (coning). Indeed, oocytes treated with 2,4-D that develop a cone show several similarities to eggs undergoing cortical contraction normally induced by fertilization (Hausen and Riebesell, 1991): contraction of the animal pole and lifting of the vitelline membrane above the plasma membrane (Fig. 1C). Underlying normal cortical contraction is a release of calcium from the endoplasmic reticulum. We are interested in examining whether calcium chelators will block the 2,4-D morphological response. Importantly, even minor changes in the cortex by 2,4-D may change the responsiveness of oocytes to progesterone by altering the accessibility or orientation of the progesterone membrane receptor. This may explain 2,4-D's ability to block key events in progesterone-induced maturation including Mos expression, MPF activation, polyadenylation of cyclin B1 mRNA and GVBD.

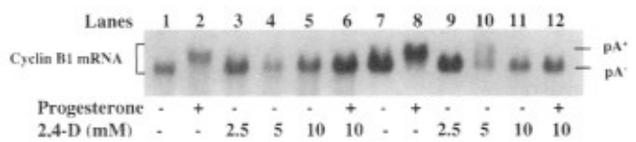

Fig. 8. Northern blot of cyclin B1 mRNA shows inhibition of cytoplasmic polyadenylation by 2,4-D. Total RNA was isolated from treated oocytes and fractionated by denaturing gel electrophoresis. Northern analysis was performed to detect the two forms of cyclin B1 mRNA, a fast migrating, nontranslated form with a short poly(A) tail labeled pA^-, and a slow migrating, translated form with a long poly(A) tail labeled pA^+. **Lanes 1–6** and **7–12** contain oocyte RNA from independent frogs.

2,4-D, itself, may act through an actin-associated receptor or signal transduction pathway, which is consistent with cytochalasin Bs ability to induce partial oocyte insensitivity. Oocyte membrane receptors for other exogenous factors, for example, muscarinic and thyrotropin-releasing hormones, show such responses (Matus-Leibovitch et al., 1993). Although we have no direct data that 2,4-D acts through a membrane receptor in oocytes, such a model is supported by our observations (not shown) that oocytes do not respond to microinjected 2,4-D.

The full-grown immature oocyte contains a store of MAPK that is activated through phosphorylation during progesterone-induced maturation downstream of Mos kinase synthesis and at approximately the same time as MPF (Palmer and Nebreda, 2000). Our results show that 2,4-D alone activates MAPK (Fig. 6), independent of Mos expression (Fig. 4) and MPF activation (Fig. 5). Interestingly, 2,4-D and other auxin-type plant hormones also induce MAPK responses in plants (Morris, 2001), which may indicate some mechanistic conservation.

In 2,4-D-treated oocytes, the immediate upstream activator of MAPK is MAPKK, as shown by our studies using the MAPKK inhibitor, U0126, which blocked MAPK phosphorylation. Since Mos, a MAPKKK, is not expressed in 2,4-D-treated oocytes, an alternative upstream activator must be involved. We postulate that MAPK activation may be a result of an independent signaling pathway that serves an essential function, to prevent the oocyte from cell cycle entry under adverse conditions. Parallel mechanisms, such as checkpoint controls, have been observed in cycling egg extracts where improper spindle formation causes the activation of MAPK, which leads to M-phase arrest (Minshull et al., 1994, Takenaka et al., 1997). Furthermore, addition of constitutively active MAPK to interphase egg extracts prevents entry into M-phase (Bitangcol et al., 1998). One possibility is that MAPK activation by 2,4-D causes the persistence of an inhibitor to M-phase entry. A similar mechanism occurs in the mature oocyte to induce metaphase II arrest whereby activated MAPK inhibits degradation of cyclin B by blocking anaphase-promoting complex (APC) (Maller et al., 2001). Alternatively, it is an intriguing possibility that MAPK could play a role as a transcriptional regulator, normally observed in interphase somatic cells (Hazzalin and Mahadevan, 2001). Although no evidence supports such a role for MAPK in oocytes under normal conditions, it remains an interesting question whether 2,4-D-activated MAPK enters the nucleus and targets transcription factors.

In conclusion, 2,4-D stimulates actin-dependent changes in pigment distribution and cell shape, and depolymerization of microtubules in full-grown *Xenopus* oocytes. Concomitantly, MAPK is activated by phosphorylation through MAPKK. Furthermore, exposure to 2,4-D blocks progesterone-induced maturation including Mos expression, MPF activation, cyclin B1 polyadenylation and GVBD, but not MAPK activation. These data suggest an independent pathway exists for 2,4-D-induced MAPK activation. We are currently examining upstream and downstream factors in this signaling pathway. Finally, although we have shown that 2,4-D prevents oocyte maturation in vitro, it is not yet clear to what extent 2,4-D and similar chemicals may negatively influence gamete formation and fertility in vivo.

ACKNOWLEDGMENTS

K.S. was supported by the Arthur A. Wilson Research Scholarship Award. Our gratitude goes to Michael Danilchik and Kim Ray at Oregon Health Science University who generously shared with us their expertise and confocal microscopy facilities. We also thank the Willamette Biology Department for its support. This research was supported by a grant from the Murdock Charitable Trust to B.S.-B.; funds from Willamette University including Atkinson Faculty Development Awards and the Science Collaborative Research Program.

REFERENCES

Andersen SSL, Bunedia B, Dominguez JE, Sawyer A, Karsenti E. 1994. Effect on microtubule dynamics of XMAP230, a microtubule-associated protein present in *Xenopus laevis* eggs and dividing cells. J Cell Biol 127:1289–1299.

Ausubel F, Brent R, Kingston RE, Moore DD, Seidman JG, Smith JA, Struhl K, Editors. 1997. Short protocols in molecular biology, 3rd Edn. New York, NY: John Wiley & Sons, Inc.

Bayaa M, Booth RA, Sheng Y, Liu XJ. 2000. The classical progesterone receptor mediates *Xenopus* oocyte maturation through a nongenomic mechanism. Proc Natl Acad Sci USA 97:12607–12612.

Bitangcol JC, Chau AS-S, Stadnick E, Lohka MJ, Dicken B, Shibuya EK. 1998. Activation of the p42 mitogen-activated protein kinase pathway inhibits Cdc2 activation and entry into M-phase in cycling *Xenopus* egg extracts. Mol Biol Cell 9:451–467.

Bradberry SM, Watt BE, Proudfoot AT, Vale JA. 2000. Mechanisms of toxicity, clinical features and management of acute chlorophenoxy herbicide poisoning: a review. Clin Toxic 38:111–122.

Cha BJ, Error B, Gard DL. 1998. XMAP230 is required for the assembly and organization of acetylated microtubules and spindles in *Xenopus* oocytes and eggs. J Cell Sci 111:2315–2327.

Charles JM, Hanley TR Jr, Wilson RD, van Ravenzwaay B, Bus JS. 2001. Developmental toxicity studies in rats and rabbits on 2,4-dichlorophenoxyacetic acid and its forms. Toxicol Sci 60:121–131.

Chesnel F, Bonnec G, Tardivel A, Boujard D. 1997. Comparative effects of insulin on the activation of the Raf/Mos-dependent MAP kinase cascade in vitellogenic versus postvitellogenic *Xenopus* oocytes. Dev Biol 188:122–133.

Ferrell JE, Jr. 1999. *Xenopus* oocyte maturation: New lessons from a good egg. Bioessays 21:833–842.

Gard DL, Cha B-J, Roeder AD. 1995. F-actin is required for spindle anchoring and rotation in *Xenopus* oocytes: A re-examination of the effects of cytochalasin B on oocyte maturation. Zygote 3:17–26.

Gard DL, Byeong JC, King E. 1997. The organization and animal-vegetal asymmetry of cytokeratin filaments in stage VI oocytes is dependent on F-actin and microtubules. Dev Biol 184:95–114.

Gaspar T, Kevers C, Penel C, Greppin H, Reid D, Thorpe TA. 1996. Plant hormones and plant growth regulators in plant tissue culture. In Vitro Cell Dev Biol Plant 32:272–289.

Gross SD, Schwab MS, Taieb FE, Lewellyn AL, Qian Y-W, Maller JL. 2000. The critical role of the MAP kinase pathway in meiosis II in *Xenopus* oocytes is mediated by $p90^{rsk}$. Curr Biol 10:430–438.

Hausen P, Riebesell M. 1991. The early development of *Xenopus laevis*. New York, NY: Springer-Verlag. pp 1–142.

Hazzalin CA, Mahadevan. 2001. MAPK-regulated transcription: a continuously variable gene switch? Nat Rev Mol Cell Biol 3:30–40.

Kaioumova D, Susal C, Opelz G. 2001. Induction of apoptosis in human lymphocytes by the herbicide 2,4-dichlorophenoxyacetic acid. Hum Immunol 62:64–74.

King ML, Zhou Y, Bubenko M. 1999. Polarizing genetic information in the egg: RNA localization in the frog oocyte. Bioessays 21:546–557.

Kosako H, Gotoh Y, Nishida E. 1994. Requirement for the MAP kinase kinase/MAP kinase cascade in *Xenopus* oocyte maturation. EMBO J 13:2131–2138.

Lilienfeld DE, Gallo MA. 1989. 2,4-D, 2,4,5-T and 2,3,7,8-TCDD: An overview. Epidemiol Rev 11:28–58.

Maller JL, Schwab MS, Roberts BT, Gross SD, Taieb FE, Tunquist BJ. 2001. The pathway of MAP kinase mediation of CSF arrest in *Xenopus* oocytes. Biol Cell 93:27–33.

Masui Y, Markert CL. 1971. Cytoplasmic control of nuclear behavior during meiotic maturation of frog oocytes. J Exp Zool 177:129–145.

Matus-Leibovitch N, Gershengorn MC, Oron Y. 1993. Differential effects of cytoskeletal agents on hemispheric functional expression of cell membrane receptors in *Xenopus* oocytes. Cell Mol Neurobiol 13:625–637.

Mendez R, Richter JD. 2001. Translational control by CPEB: A means to an end. Nat Rev 2:521–529.

Merriam RW, Sauterer RA, Christensen R. 1983. A subcortical, pigment-containing structure in *Xenopus* eggs with contractile properties. Dev Biol 95:439–446.

Minshull J, Sun H, Tonks NK, Murray AW. 1994. A MAP kinase-dependent spindle assembly checkpoint in *Xenopus* egg extracts. Cell 79:475–486.

Morris PC. 2001. MAP kinase signal transduction in plants. New Phyt 151:67–89.

Nebreda AR, Hunt T. 1993. The c-*mos* proto-oncogene protein kinase turns on and maintains the activity of MAP kinase, but not MPF, in cell-free extracts of *Xenopus* oocytes and eggs. EMBO J 12:1979–1986.

Palmer A, Nebreda AR. 2000. The activation of MAP kinase and p34cdc2/cyclin B during the meiotic maturation of *Xenopus* oocytes. Prog Cell Cycle Res 4:131–143.

Reinsch S, Gönczy P. 1998. Mechanisms of nuclear positioning. J Cell Sci 111:2283–2295.

Resing KA, Mansour SJ, Hermann AS, Johnson RS, Candia JM, Fukasawa K, Vande Woude GF. 1995. Determination of v-Mos-catalyzed phosphorylation sites and autophosphorylation sites on MAP kinase kinase by ESI/MS. Biochemistry 34:2610–2620.

Rosso SB, Caceres AO, Evangelista de Duffard AM, Duffard RO, Quiroga S. 2000. 2,4-Dichlorophenoxyacetic acid disrupts the cytoskeleton and disorganizes the Golgi apparatus of cultured neurons. Toxicol Sci 56:133–140.

Ryabova LV, Vassetzky SG. 1997. A two-component cytoskeletal system of *Xenopus laevis* egg cortex: Concept of its contractility. Int J Dev Biol 41:843–851.

Schettler T, Solomon G, Valenti M, Huddle A. 1999. Generations at risk: Reproductive health and the environment. Cambridge, MA: MIT Press. pp 1–417.

Shiina N, Moriguchi T, Ohta K, Gotoh Y, Nishida E. 1992. Regulation of a major microtubule-associated protein by MPF and MAP kinase. EMBO J 11:3977–3984.

Sitbon F, Perrot-Rechenmann C. 1997. Expression of auxin-regulated genes. Physiol Plant 100:443–455.

Smith LD, Ecker RE. 1971. The interaction of steroids with *Rana pipiens* oocytes in the induction of maturation. Dev Biol 25:232–247.

Stebbins-Boaz B, Richter JD. 1997. Translational control during early development. Crit Rev Eukaryot Gene Expr 7:73–94.

Stebbins-Boaz B, Hake LE, Richter JD. 1996. CPEB controls the cytoplasmic polyadenylation of cyclin, Cdk2, and c-Mos mRNAs and is necessary for oocyte maturation in *Xenopus*. EMBO J 15:2582–2592.

Taieb F, Thibier C, Jessus C. 1997. On cyclins, oocytes and eggs. Mol Reprod Dev 48:397–411.

Takenaka K, Gotoh Y, Nishida E. 1997. MAP kinase is required for the spindle assembly checkpoint but is dispensable for the normal M phase entry and exit in *Xenopus* egg cell cycle extracts. J Cell Biol 136:1091–1097.

Tian J, Kim S, Heilig E, Ruderman JV. 2000. Identification of XPR-1, a progesterone receptor required for *Xenopus* oocyte activation. Proc Natl Acad Sci USA 97:14358–14363.

Tuschl H, Schwab C. 2003. Cytotoxic effects of the herbicide 2,4-dichlorophenoxyacetic acid in HepG2 cells. Food Chem Toxicol 41:385–393.

Zhao Y, Li W, Chou I-N. 1987. Cytoskeletal perturbation induced by herbicides 2,4-dichlorophenoxyacetic acid (2,4-D) and 2,4,5-trichlorophenoxyacetic acid (2,4,5-T). J Toxicol Environ Health 20:11–26.